Environ Geol (2007) 52:1399–1412
DOI 10.1007/s00254-006-0582-9

ORIGINAL ARTICLE

Development and parameterisation of a complex hydrogeological model based on high-resolution direct-push data

B. Miles · T. Kalbacher · O. Kolditz · C. Chen · J. Gronewold · W. Wang · A. Peter

Received: 14 July 2006 / Accepted: 5 November 2006 / Published online: 27 January 2007

Abstract Ongoing developments in geological and hydrogeological investigation techniques, especially direct-push methods, have led to an increase in the quality, density and spatial resolution of data available from such investigations. This has created new challenges in the development of numerical models in terms of accurately and efficiently translating detailed and complex conceptual models into effective numerical models. Suitable geometrical and numerical modelling tools are essential in order to meet these challenges. This paper describes the development of a three-dimensional hydrogeological flow model for a contaminated site near Berlin, Germany, based on high-resolution geological data obtained principally using direct-push methods. The available data were first interpreted to construct a detailed GIS-based geological model, which formed the basis of the conceptual site model. The conceptual model was then translated into a geometrical model, which was used to create a finite element numerical model. An innovative geometry object-based approach enabled the complex structural details of the conceptual model to be accurately reproduced in the numerical model domain. The resulting three-dimensional steady-state unconfined flow model was successfully calibrated using external automated calibration software, whereby parameter values for groundwater recharge and hydraulic conductivity were determined.

Keywords Groundwater modelling · High-resolution data · Parameter optimisation · Geometrical model · Direct-push

B. Miles (✉) · A. Peter
Tuebingen Groundwater Research Institute (TGF),
c/o Center for Applied Geosciences,
University of Tuebingen, Sigwartstr. 10,
Tuebingen 72076, Germany
e-mail: ben.miles@uni-tuebingen.de

T. Kalbacher · O. Kolditz · C. Chen ·
J. Gronewold · W. Wang
Center for Applied Geosciences,
University of Tuebingen,
Sigwartstr. 10, Tuebingen 72076, Germany

Introduction

The ongoing development and improvement of geological and hydrogeological investigation methods, in particular direct-push methods, has led to an increase in the quality, density and spatial resolution of data available from such investigations. This development is of particular relevance when considering contaminated sites, where numerical models play an increasingly important role in site assessment and management plans. With detailed geological data and high-resolution groundwater sampling, an increased level of detail is called for in both conceptual site models and numerical flow and transport models. As the complexity of conceptual and structural models increases, innovative approaches and techniques are required to fully exploit the available data, both in the generation of structural models and particularly in the translation of the conceptual and structural models into effective numerical models. Often complex structures need to be defined in the numerical model domain with a high degree of spatial accuracy, presenting a significant challenge. The finite element approach is well suited to the problem of representing complex structures,

offering a greater degree of flexibility than a regular finite difference grid.

This paper presents the development and calibration of a three-dimensional finite element steady-state unconfined groundwater flow model for a contaminated site near Berlin, Germany. The site, a former military airfield heavily contaminated with kerosene aviation fuel, is a research site for the natural attenuation of petroleum hydrocarbons. The calibrated groundwater flow model is intended to provide hydrogeological parameters and boundary conditions for a reactive transport modelling study of the natural attenuation processes at the site, for which a sound understanding of the hydrogeological situation is a fundamental requirement. The complex quaternary geology at the site is well characterised through a dense network of direct-push soundings (whereby a probe is driven or hammered into the subsurface to collect data or install a small diameter monitoring well) and drilling logs from conventional wells, from which a detailed three-dimensional GIS-based structural model was created. The GeoSys/RockFlow finite element model code (Kolditz et al. 2006) was used to create a numerical site model from the GIS-based structural site model in an innovative approach using geometrical entities to map the structural model and boundary conditions, and source terms for the conceptual hydrogeological model onto a finite element mesh. In particular for the later reactive transport modelling, it was desirable to include small-scale features identified in the interpretation of the geological data in the flow model. The resulting steady-state flow model was calibrated to the measured hydraulic heads at the site using the automated calibration software PEST (Doherty, 2004), whereby values for groundwater recharge rates and for hydraulic conductivity were identified.

Site description

Flughafen Brand, shown in Fig. 1, is a disused military airfield located approximately 60 km south of Berlin, Germany, in the state of Brandenburg. First established as a military airfield at the end of the nineteenth century, from 1945 until its closure in 1992 the site was under the control of the Russian military. During this time there was massive contamination of the ground beneath the fuel handling and storage facilities. Today the subsurface is contaminated over an area of approximately 110 ha with kerosene jet fuel, which to a large extent is present as a mobile non-aqueous phase in the capillary fringe.

The site lies in a topographically flat region of Pleistocene glacial sediments, with a local elevation of around 60 m above sea level. Hydrologically, the site is located in the Spree river catchment, a small creek approximately 2.5 km to the West being the nearest surface water feature. The geology at the site consists of quaternary sediments of up to 100 m in thickness with principal units of medium, coarse and fine sand. The stratigraphy is complex, forming a hydraulically connected system of aquifers extending to the base of the sediments. Intermediate discontinuous layering of silt and clay is found in the parts of the uppermost aquifer and unsaturated zone. The silt layers are in places glacially deformed with highly variable topography and in parts of the site form the aquitard of a perched aquifer. The unsaturated zone at the site is approximately 13 m in thickness, with the groundwater table typically around 48 m above sea level.

A number of investigations have been carried out at the site since the transfer of ownership to the state of Brandenburg in 1992. For the hydrogeological characterisation a total of 37 conventionally bored groundwater monitoring wells and fifty 1 in. direct push multi-level monitoring wells are available, with groundwater levels measured on a monthly basis since April 2005. The geological survey of the site consists of the drilling records for the conventional wells, as well for the 93 cone penetrameter (CPT) soundings and 15 electrical conductivity soundings. The locations of the sounding points and monitoring wells are shown in Fig. 1. Additionally, a total of 11 samples of aquifer material have been taken at ten different locations. These were used both to support the interpretation of data from the direct-push soundings, as well as for the determination of porosity and the estimation of hydraulic conductivities based on particle size distributions. Hydraulic conductivities were also determined in-situ from slug tests carried as part of ongoing site investigations after the hydrogeological model was completed, yielding values which compare favourably with the values determined in the model calibration (see section ''Optimised parameters'').

Conceptual site model

The conceptual site model in this case comprises a three-dimensional geological model of the saturated zone and a hydrogeological conceptual model. The following sections detail the interpretation of the field data and the respective development of these two models.

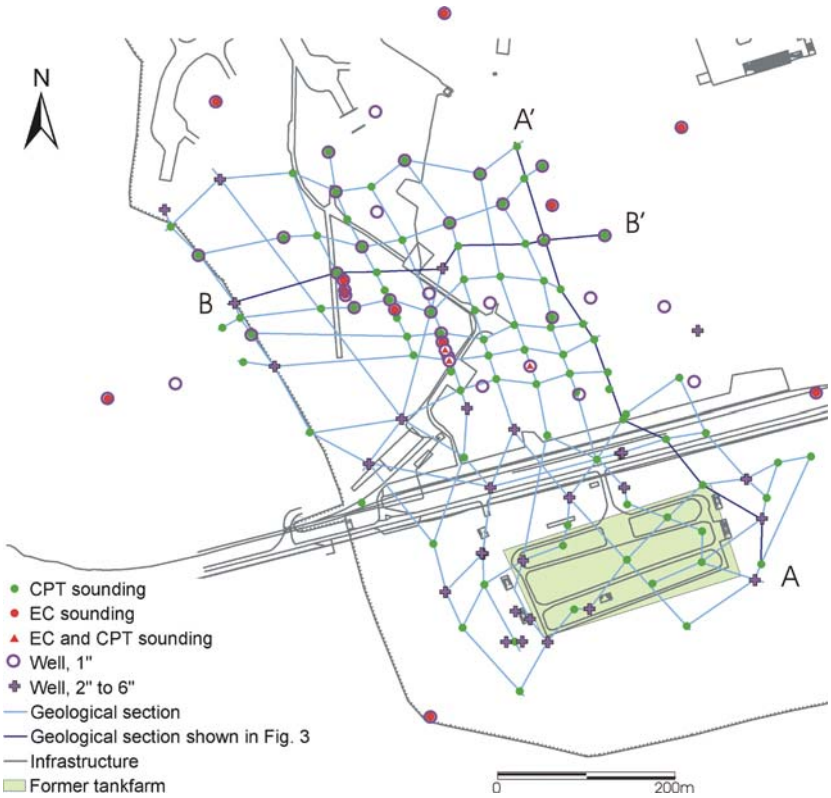

Fig. 1 Site map showing locations of monitoring wells, geophysical sounding points and geological profiles used in the development of the structural model

Interpretation of geological data

Geological data for the site were available in a number of forms, both from samples of aquifer material and drilling logs from the installation of conventional monitoring wells, as well as from direct push cone penetrometer (CPT) and electrical conductivity (EC) soundings.

The following section will briefly summarise the information available from the various methods, and describe the combination of the various data in the structural model for the site.

Soil cores and drilling logs provide direct geological information, however—unless a continuous core sample is taken, which is generally an expensive exercise—with poor vertical resolution. Smaller scale hydrostratigraphic features, which can be of particular interest and importance with relation to contaminant transport, generally cannot be delineated. Direct push methods, whereby a probe is driven or hammered into the subsurface, generally deliver data at a higher vertical resolution. Additionally they are typically faster, and hence cheaper, than conventional drilling methods; thus a higher density of sampling locations is possible in a site investigation.

The cone penetrometer test is probably the most well established of all direct-push sounding methods, and dates back to the 1920s. The penetrometer itself essentially consists of a cone-shaped probe at the end of a steel shaft. Sensors in the probe measure the mechanical resistance at the tip and sleeve friction along the shaft as the probe is driven into the subsurface at a constant rate. From the tip resistance and sleeve friction the sediment type can be inferred (Robertson 1990). Sand, for example, typically has a high tip resistance and low sleeve friction, whereas a till has a low tip resistance and high sleeve friction (Robertson and Campanella 1983a, b). The data from a CPT sounding can thus be interpreted to provide a profile of the sediment progression with a vertical resolution in the order of 0.02 m. Such an interpretation is shown in Fig. 2, whereby the relationship between tip resistance, sleeve friction and the inferred material type can be clearly seen. At locations where 1.2 m length soil cores corresponding with the CPT soundings were available, a good agreement was found between the CPT interpretation and the material in the core.

In a direct push EC sounding a conductivity probe is driven into the subsurface, while the apparent electrical conductivity of the sediments is calculated from an imposed electrical current (Dietrich and Leven 2005). The probe itself typically has four electrodes in a Wenner array, whereby the electrodes are arranged in

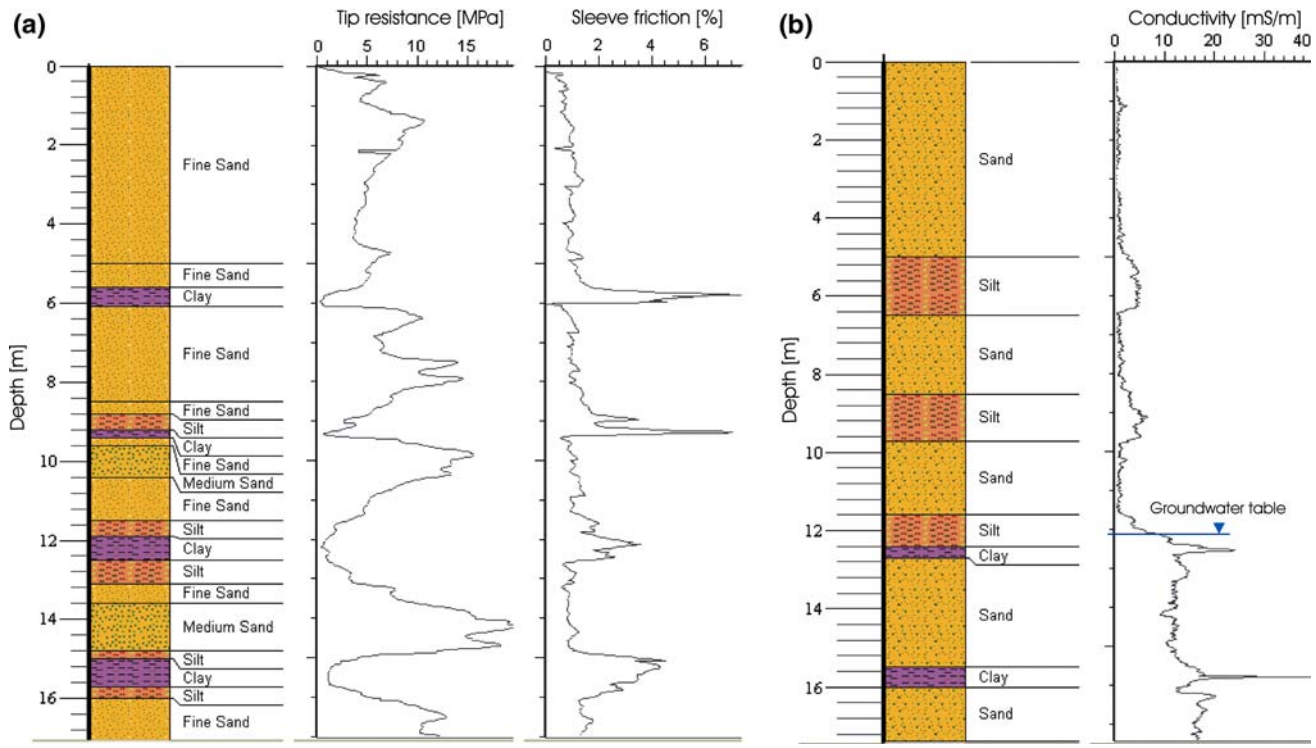

Fig. 2 Geological profiles **a** from interpretation of CPT data **b** from interpretation of EC data at the same location

a line; a current is driven through the soil between the two outer electrodes and a voltage measured across the inner electrode. The electrical conductivity of sediments in the saturated zone of an aquifer where variations in groundwater chemistry are small is principally controlled by particle size and mineral type, with clay minerals having a higher conductivity than sands. For sediments with a low electrical conductivity, such as sands, an increase in conductivity is generally observed at the groundwater table, the magnitude of the increase being a site-specific parameter dependant on groundwater chemistry. Thus zones of low hydraulic permeability can be identified in the vertical profile (Schulmeister et al. 2003). The vertical resolution of the data collection depends on the spacing of the electrodes in the probe; using a Geoprobe® direct push unit and conductivity probe, data were recorded with a vertical resolution in the order of 0.02 m. A typical profile obtained for the site is shown in Fig. 2.

Comparing the geological interpretations for the CPT and EC soundings in Fig. 2 it can be seen that there is a good agreement between the two methods in terms of defining the positions of the low permeability units. There are, however some discrepancies in the interpretation of the material type of these units; where the CPT interpretation indicates clay, the EC interpretation is silt and vice-versa. This is because the interpretations for both methods are based principally on empirical relationships, and are to some extent subject to the influence of site-specific factors. The overall increase in conductivity at the groundwater table can clearly be seen in the EC profile between 11.5 and 12 m below the surface.

The combined data from the drilling logs, CPT and EC soundings, which were also compared with undisturbed soil samples, where available, were used to prepare 24 intersecting two-dimensional geological profiles for the site in a GIS-based environment. Five material classes were used in the geological interpretation: fine, medium and coarse sand, silt and clay, to which hydrogeological parameters were also assigned (see section ''Calibration parameter ranges''). The locations of the profiles can be seen in Fig. 1, and an example of two intersecting profiles is shown in Fig. 3.

Development of the 3D geological model for the saturated zone

The 2D geological profiles were divided into layers, with top of the uppermost layer at approximately 50 m above sea level, slightly above the average groundwater level for the site. Where possible, the layers were arranged such that the typically discontinuous patches of different sand types and discrete units, such as silt lenses, were defined within a single layer. This resulted in nine layers of varying thickness over a total depth of

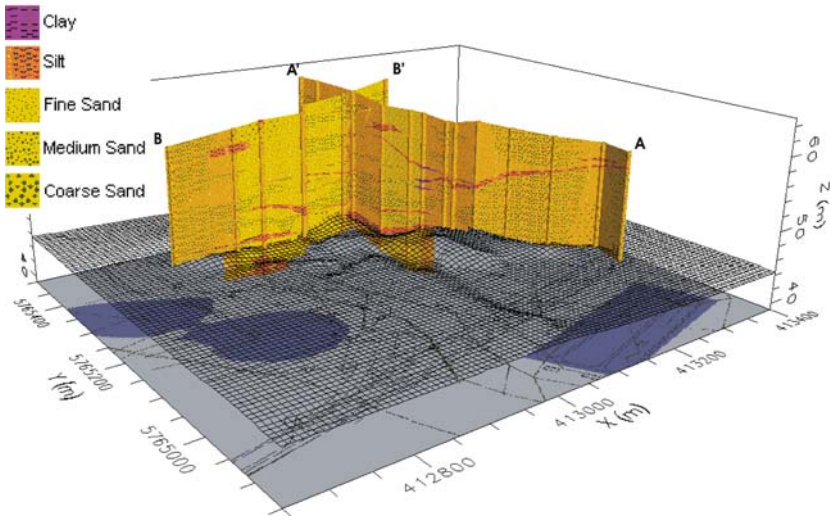

Fig. 3 Intersecting two-dimensional geological profiles (see Fig. 1 for the profile locations). The *wire mesh surface* shows a laterally interpolated layer

approximately 11 m. Three-dimensional surfaces were then created by interpolating the layer elevations between the two dimensional profiles (see Fig. 3). The geological information at each layer interface in the 2D profiles was then interpolated laterally between the profiles, creating maps of the distribution of different material types within each of the layers. These material distribution maps were then imposed on the layer elevation surfaces to create three-dimensional volumes delineating the material types, using methods described subsequently in the sections GIS interface and methods and Mapping procedure.

Development of the conceptual hydrogeological model

Hydraulic head data recorded at monthly intervals at the site show only minor fluctuations in the local flow field in the short to medium term. On this basis, a steady-state flow model for the site was developed. For the development and calibration of the model the most recent, and in terms of observation density the most comprehensive, set of measurements, namely from December 2005 was used. Figure 4a shows the hydraulic situation and the model domain. The groundwater flow at the site is from South to North, and generally divergent. As the divergent flow pattern in the area cannot be directly attributed to local topographical or hydrological features, it is thought that it may be due to secondary perched aquifer systems collecting infiltrating water and focussing it in small areas where there is communication with the main aquifer, causing localised changes in the hydraulic gradient. This explanation was subsequently supported by the hydrogeological model. The domain covers an area significantly larger than that of interest for later reactive transport modelling in order to minimise boundary effects. As the area lacks geological, hydrogeological and hydrological features that might lend themselves to the definition of model boundaries, these were based on interpolated hydraulic head isolines. At the upstream and downstream boundaries (here corresponding to South and North, respectively) a fixed head condition is applied. The upstream boundary was assigned a value of 50.38 m along its entire length. For the downstream boundary, which spans a much greater length, the fixed head value was varied between 49.65 and 49.75 m along the boundary, following the trend of the northernmost isolines. The no-flow boundaries to the East and West are normal to the head isolines at the points where they intersect.

The zonation of groundwater recharge in the model domain into ten zones, as shown in Fig. 4b, was based on a combination of the geological situation and the surface ground cover. The ground cover at the site, which directly affects local groundwater recharge through its influence on infiltration and evaporation, can be seen in Fig. 4b. The cover can be classified as areas of mixed forest, sealed surfaces related to the former military infrastructure, bare ground, sparse scrub and brush. Additionally there is a large unsealed landfill, about which little is known. In the southern half of the site a basin-shaped silt structure in the unsaturated zone forms the aquitard of a perched aquifer. The extent of this feature, delineated from the available geological information, can be seen in Fig. 4b, while a three-dimensional visualisation of the structure is shown in Fig. 4c. The assumed flow direction for water in this structure is from East to West. At two points along the northern boundary of the perched aquifer, the edge of the silt aquitard is at a lower elevation than the minimum measured groundwater level

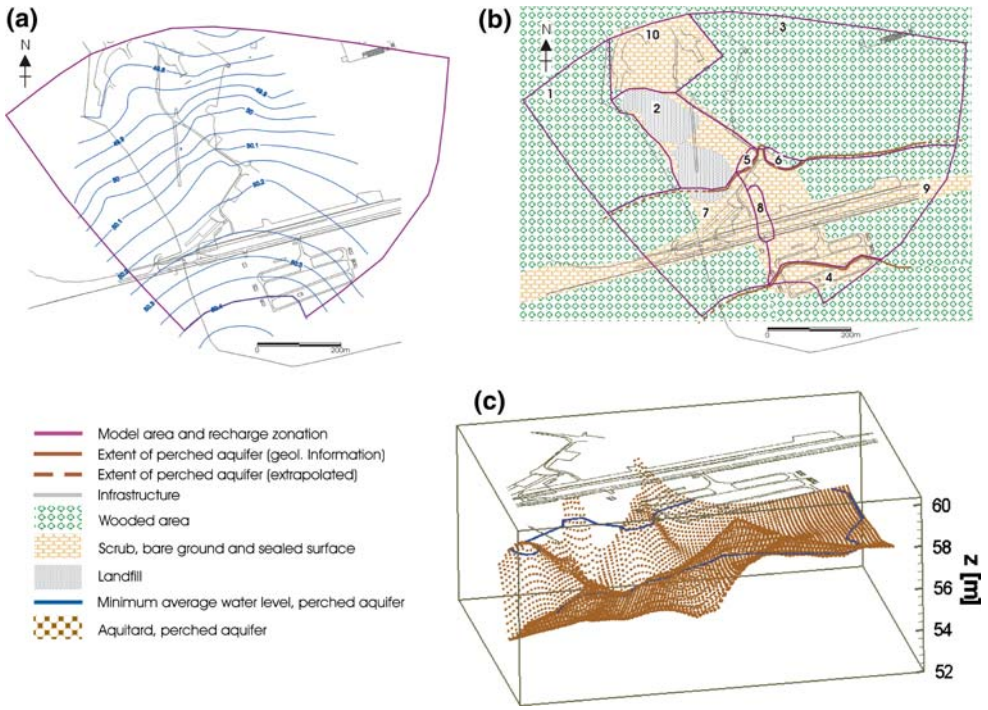

Fig. 4 **a** Model area based on measured head values; **b** numbered recharge zones with approximate ground cover distribution and the extent of the perched aquifer in the southern half of the site; **c** 3D-visualisation of the perched aquifer, showing the basin form of the aquitard and the minimum water level

in the upper aquifer, and it is thought that at these points there may be an overflow to the lower aquifer. In the central region of the basin structure, discontinuities in the silt layers are thought to act as windows, communicating to some extent with the lower aquifer. The perched aquifer is thought to significantly influence the distribution of groundwater recharge at the site by intercepting and gathering recharge across a large area in the southern part of the site and focussing it to some extent at these points. The selection of parameter values for the hydrogeological conceptual model is discussed in the section Calibration parameter ranges.

Numerical site model

The generation of the numerical site model from the conceptual model required the use of various computational methods and brings together geometrical, topological and process related data. New object-oriented software methods have been developed for this purpose. Three object libraries are used in GeoSys/Rockflow to handle geometrical (GEO objects, GIS interface and methods), topological (MSH objects, Domain discretization) and numerical operations for process (i.e. hydraulic) simulations (PCS objects, Process model). The organisation of the object libraries is depicted in Fig. 5. The volume and high resolution of the data from the Brand field site required the development of methods for efficient data processing, including GUI (graphical user interface) and 3D visualization tools, in order to make the available data accessible for process analysis (Fig. 5).

GIS interface and methods (GEO objects)

For the generation of the numerical model, GIS-based data from the conceptual site model was imported directly in ESRI shape file format (ESRI 1998) via a GIS data interface implemented in the GeoSys/RockFlow code (Chen 2006). This enabled the automated generation of the GEO objects (points, polylines, surfaces, volumes and domains) required to make the data from the structural model available for the numerical model. In this way, data for the following aspects of the numerical model could be imported from the conceptual model;

- Domain properties (see section ''Domain discretization''): the initial geometric input for the domain discretization.
- Node properties (see section ''Assignment of process data''): location of initial conditions, boundary conditions and source sink terms.
- Element properties (see section ''Assignment of process data''): spatial distribution of the material properties to be assigned to the finite elements.

The laterally interpolated geological information for the layers of the 3D geological model (see Develop-

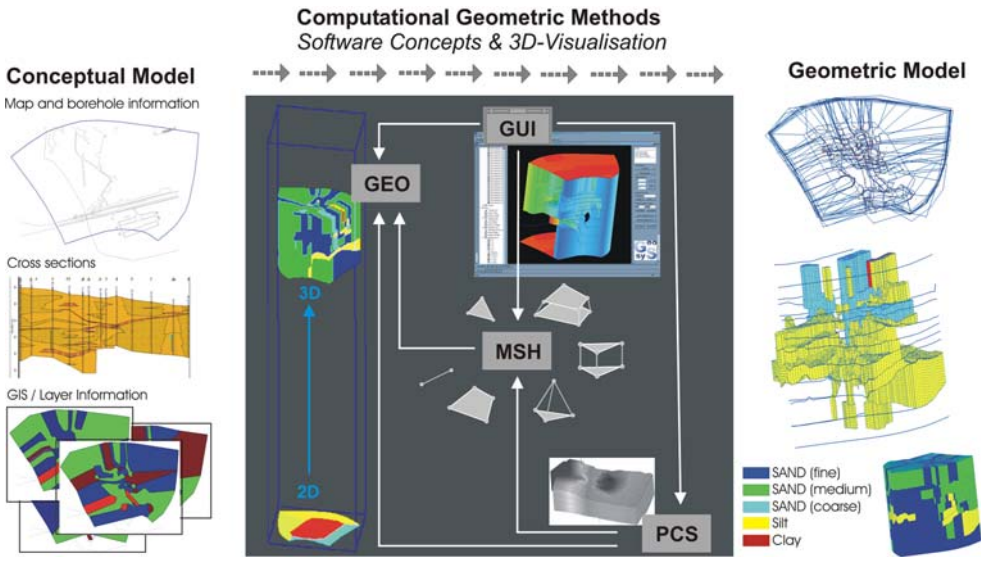

Fig. 5 Computational geometric methods in combination with 3D-visualisation enabling the translation of conceptual model information to the geometrical model (Kalbacher 2006)

ment of the 3D geological model for the saturated zone) was imported as a series of GIS raster maps. These were mapped to their corresponding interpolated layer elevations using the mapping procedure described below; thus defining the 3D volume objects used in the construction of the 3D structural model.

Domain discretization (MSH objects)

Discretization of the model domain as a mesh consisting of nodes connected by elements is a fundamental part of the finite element model (FEM) analysis process. The quantity and quality of the finite elements influence the accuracy, convergence and speed of the groundwater model solution. Locally refined triangulations were used to allow accurate approximation of the complex geological structural model. Based on the surface triangulation, structured prism elements were first generated for each layer, and then adjusted based on layer elevation raster maps (Fig. 6, TIN-Layers). Within GeoSys/Rockflow, data and methods for meshing purposes are organised in an object library, MSHLib, which is dependant on GEO objects (Fig. 5).

Mesh generation

In this application, an unstructured 2D triangular mesh was first generated for a polygonal 2D surface representing the model domain area (see Development of the conceptual hydrogeological model). This was then extended to a structured 3D prismatic mesh based on the 3D layer interface elevations from the geological model (see Development of the 3D geological model for the saturated zone). For the initial domain triangulation (Fig. 6a), a mesh generator based on an unstructured 2D Delaunay Algorithm (Shewchuk 1996) implemented in the GMSH code (http://www.geuz.org/gmsh/) was used. The density distribution of the thus created 2D triangle mesh follows specific element size definitions at points of the bounding segments. An element size definition at each geometric point is essential before starting the mesh generation. The element size allocation must take user-defined density distribution as well as the geometrically required element sizes (i.e. distance to neighbour points) into account to ensure an appropriate mesh quality. A 2D surface made up of five polygons was used to generate a mesh with an increased density distribution in the central region of the model domain. A density distribution value of 10 m was assigned for the central region of the model domain, and a value of 15 m for the outer regions. The resulting decreased element size in the centre of the mesh compared to the outer regions was intended to take account of the higher density of geological data available, and hence level of detail in the structural model in this region.

The 2D triangulation provided the initial mesh for the structured 3D prism generation (Fig. 6a). The prism generator was designed to extend 2D triangulated meshes to layered 3D models. The algorithm creates an initial prism layer from the 2D mesh and then translates copies of this layer stepwise ''under'' (here in z-direction) the previous prism layer. The prism mesh is thus derived from the unstructured triangle mesh and each of the underlying elements inherits the element quality of the original triangle.

The prismatic mesh used for the numerical site model contained 52,330 nodes connected by 92,727 elements in nine prism layers.

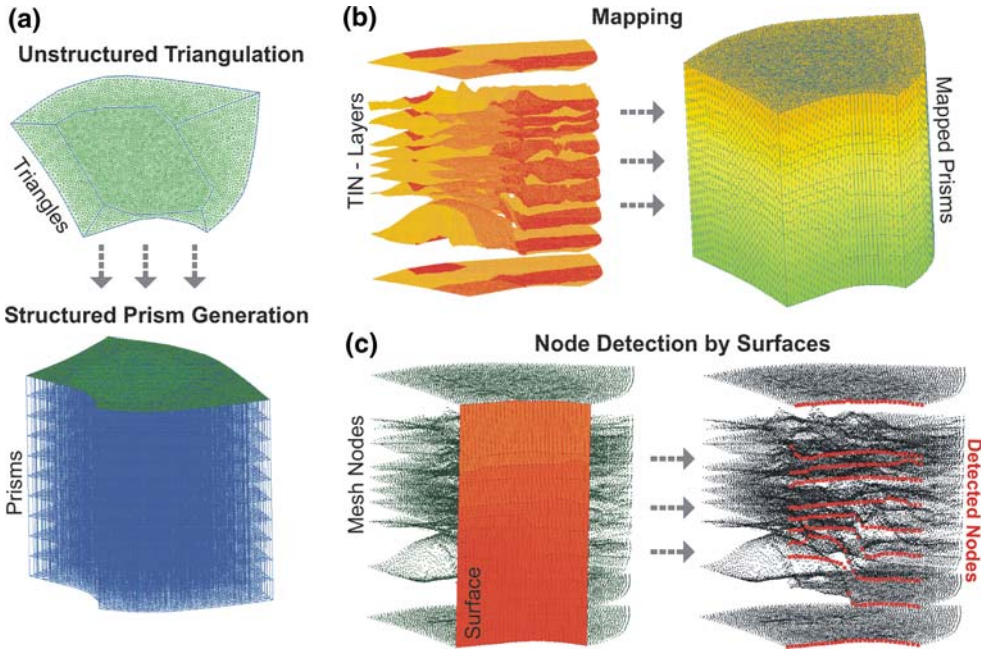

Fig. 6 **a** The triangulation process considers the polygonal input data, and prism meshes can be created in a structured way based on unstructured 2D meshes. **b** Such prism meshes can be mapped by appropriate triangulated irregular networks (TIN). **c** Search algorithms are able to detect mesh nodes that lie on a surface, here for the downstream boundary condition nodes. The pictures are exaggerated vertically for clarity ($Z \times 100$)

Mapping procedure

The mapping of the prism layers is a procedure to position (vertical height) and modulate the prism elements according to topographic and stratigraphic information, which is provided by TIN or grid files (Fig. 6b). Suppose a layer surface is defined by a regular grid on a horizontal plane with an elevation at each of its nodes, together with a 2D mesh parallel to the horizontal plane (see Fig. 7, left). Considering the horizontal plane is parallel to the plane of (x, y, 0) in the Cartesian system, the task of mapping is to move each node of the 2D mesh to the given surface without changing the x and y components of its coordinates (Fig. 7, right). The mapping approach is very simple. For each node n, we first locate the block in the grid with four grid points, e.g. i, j, k, l, and this block contains node n (Fig. 7, left). The block can then be considered as a quadrilateral finite element with nodes, i, j, k, l. Next, the local coordinate (ξ, η) of node n and corresponding values of the four finite shape functions N_i, N_j, N_k and N_l are calculated. Assuming the elevations of the four points are z_i, z_j, z_k, z_l, the final step of the mapping is to interpolate a new z of n by

$$z_n = z_i N_i + z_j N_j + z_k N_k + z_l N_l$$

Using this method, the prismatic mesh layers were mapped to the interpolated layer elevations generated in the geological model of the saturated zone.

Process model (PCS objects)

In this section the mathematical model and the numerical approximation scheme as well as the technical part of model parameterisation are briefly de-

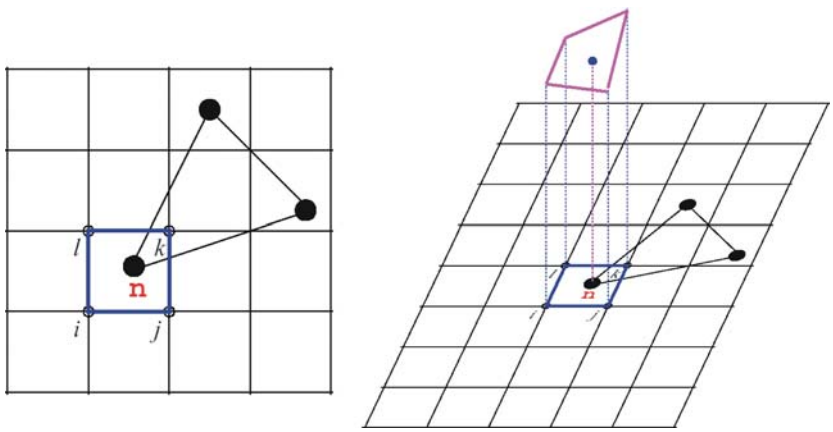

Fig. 7 Node of an element in the grid (*left*), and mapping an element node to the surface

scribed. Due to the geometric complexity of the Brand case a new combination of GIS and database methods were developed for assigning parameters to the discretised numerical model.

Governing equations

The present work considers steady-state groundwater flow in an unconfined aquifer, which is a non-linear problem using hydraulic head h as the primary variable. In the unconfined flow approach, a capillary fringe is not considered and the water table defines the boundary between the unsaturated and saturated zones. Unconfined flow is treated as a free surface problem, with the water table defined as a surface where the liquid pressure is assumed to be equal to the atmospheric air pressure. To model unconfined flow a moving mesh technique is used (Beinhorn 2005). According to Bear (1972) the mass balance equation for a fluid phase (i.e. groundwater) is given by

$$S_0 \frac{\partial h}{\partial t} + \nabla \cdot \mathbf{q} = Q_\rho \tag{1}$$

with the specific storativity of the porous medium S_0, the Darcy flux $\mathbf{q}$ and a source term for fluid mass Q_ρ. Unconfined flow conditions are mimicked by a kinematic boundary condition at the ground water table surface.

$$h = z|\text{groundwater table} \tag{2}$$

with the elevation of the groundwater table z. Darcy's equation is given by

$$\mathbf{q} = -\mathbf{K}\left(\frac{\nabla h - \rho - \rho_0}{\rho_0}\frac{g}{g}\right) \tag{3}$$

with the hydraulic conductivity tensor $\mathbf{K}$, the fluid density ρ and a corresponding reference value ρ_0, the gravity vector g and the value of gravity acceleration $g = 9.81\ \text{ms}^{-2}$.

Numerical model

The method of weighted residuals is applied to derive the weak formulation of the fluid mass balance equation (1). Assume that $V_n \subset H_1\ \Gamma\ (\Omega)_n$ is the test function space. For all $\omega \subset V_1$, we have the weak form of the mass balance equation (1) as

$$\int_\Omega \omega\left(S_0 \frac{\partial \hat{h}}{\partial t} + \nabla \cdot \mathbf{q} - Q_\rho\right) d\Omega = 0 \tag{4}$$

with the finite element domain Ω, the test functions ω, the hydraulic head approximation $\hat{h}$. Applying integration by parts, Eq. (4) can be rewritten as

$$\int_\Omega \omega\left(S_0 \frac{\partial \hat{h}}{\partial t}\right) d\Omega + \int_\Omega \omega(\nabla\omega \cdot \mathbf{q}) d\Omega - \int_\Omega \omega Q_\rho d\Omega = -\int_\Gamma \omega(\mathbf{q} \cdot \mathbf{n}) d\Gamma \tag{5}$$

with the domain border for Neumann type boundary conditions Γ. We use the Galerkin finite element method to solve the weak forms of fluid mass balance equation (5), i.e. test functions and element shape functions are set identically. The hydraulic head variable is approximated by admissible finite element functions.

$$\hat{h} = \sum_i^n h_i(t) N_i(\mathbf{X}) \tag{6}$$

with element node index i, number of nodes per element n, nodal head values h_i which are time dependent and nodal shape functions N_i which are space dependent. As a result of the finite element procedure an algebraic equation system is derived.

$$\mathbf{A}\mathbf{h}^{n+1} = \mathbf{b} \tag{7}$$

with the global system matrix $\mathbf{A}$, the nodal hydraulic head vector $\mathbf{h}$ at new time level $n + 1$, and the right-hand-side vector $\mathbf{b}$. Local element matrices and vectors are calculated and then assembled from all elements e to the global system matrix,

$$\mathbf{A} = \frac{1}{\Delta t}\sum_e \int_{\Omega^e} N S_0 N^T d\Omega^e + \theta \sum_e \int_{\Omega^e} \nabla N \mathbf{K} \nabla N^T d\Omega^e \tag{8}$$

as well as the global right-hand-side vector

$$\mathbf{b} = \frac{1}{\Delta t}\left(\sum_e \int_{\Omega^e} N S_0 N^T d\Omega^e\right)\mathbf{h}^n - (1-\theta) \times \left(\sum_e \int_{\Omega^e} \nabla N \mathbf{K} \nabla N^T d\Omega^e\right)\mathbf{h}^n + \sum_e \int_{\Omega^e} N Q_\rho d\Omega^e - \sum_e \int_\Gamma N(\mathbf{q} \cdot \mathbf{n}) d\Gamma \tag{9}$$

with the time step increment Δt, old time level n, and collocation factor θ.

In the framework of the object-oriented FEM, instances of a general finite element class CFiniteElement for parabolic PDE types deal with all related FE operations, such as element matrix calculations and global assembly, for arbitrary geometric element types (Wang and Kolditz 2006).

Assignment of process data

The assignment of process (PCS) data is the final step before numerical simulations can be performed. PCS data can be subdivided into node- and element-related properties. Node-related process data are the source terms, initial conditions and boundary conditions, which have to be assigned to mesh nodes. Element-related process data are the material properties, which have to be assigned to mesh elements.

The large mesh constructs which result from detailed and complex real three-dimensional hydrogeological models effectively preclude manual parameter and property assignments. An alternative is the management of data sets in combination with the ''basic'' geometry (e.g. Kalbacher et al. 2006; Chen 2006), which is provided by the GEO objects. Generally, the approach of basing the assignment of node and element properties on the GEO objects has the advantage that changes to the structural or conceptual model, which are then transferred to the numerical model via these objects, are made completely independent of the finite element mesh, and vice-versa.

Node properties

Geometrically, boundary conditions can be defined by points, polylines and surfaces. Here, the boundary conditions were defined as surfaces, which were used to detect the mesh nodes to which the boundary conditions should be assigned for the groundwater flow model (Fig. 6c). These surfaces were triangulated using the Delaunay algorithm and passed to TIN vector constructs of the GEO objects. An initial node selection is achieved by creating a bounding box around the surface and transferring the points to a local vector construct. This substantially reduces the number of iterations required in the second step, whereby each triangle is used to detect the nodes located inside the triangle or on its edge. Detected nodes are marked in the node vector construct of the mesh and the located nodes of the local node vector are deleted, resulting in an additional reduction in computation time. The same approach was used to apply source terms for groundwater applied to the nodes of the top layer of the model domain. The advantage of physical assignment by basic and mesh independent geometric entities is their fast creation. However, it should be stressed that a visual check is still very important to ensure the reliability.

Element properties

Values for material physical properties in the model are assigned to the elements of the mesh according to the spatial distribution of the materials (see GIS interface and methods). The parameter data thus have two characterizing features: their numerical value and their spatial distribution. Parameter values for the material groups were imported interactively using a pre-prepared database template which allowed the imported values to be assigned directly to their corresponding geometric objects (Gronewold 2006). The connections produced in this way are saved as material groups (MAT). Using the volume or surface definitions, search algorithms similar to those used for the node property detection locate the relevant mesh elements and assign the appropriate material group properties to them.

Inverse modelling approach and parameter identification

The application of automated model calibration tools for parameter estimation in inverse models and the advantages of such an approach have been described in numerous publications (Carrera and Neuman 1986; Hill 1992, 1998; Poeter and Hill 1997). Briefly, the main benefit of such an approach is its ability to optimise the base model, determining parameter values that provide a quantified best fit between simulated model output and measured data. The parameters optimised were hydraulic conductivities and recharge rates, using measured head values from December 2005 as the calibration target.

Implementation of the PEST parameter estimation tool

The parameter estimation software, PEST (Doherty 2004) was chosen for the model calibration and parameter identification. The latest version of the software, v10.0.2, October 2005, was used. The estimation technique adopted by PEST has been tested on a wide range of problems and is considered to be quite robust (Doherty, 2004). The software could be directly applied to the GeoSys/RockFlow model code by preparing template files corresponding to the model's text format input and output files, using the methods described in the PEST software documentation (Doherty 2004).

Objective function

The goal of any model calibration is to minimise the difference between a set of observed values and values generated by a model. The PEST code computes values for a set of parameters that minimise the objective function, Φ, which is essentially the sum of the squared differences between modelled and observed values. The software iteratively analyses the influence on the objective function for changes in each of the parameters to be optimised and then adjusts the parameters to achieve a maximum reduction in Φ. The mathematics of the PEST algorithm are comprehensively described in the software documentation (Doherty 2004). Briefly, the basis for the non-linear parameter estimation is the assumption that the modelled system can be represented by a continuously differentiable function, M, which maps n-dimensional parameter space into m-dimensional observation space, described by:

$$h_o = M(\boldsymbol{p}_o) \tag{10}$$

where $\boldsymbol{p}_o$ is the vector representing the set of parameters and h_o the set of model calculated observations. A further set of model calculated observations can be calculated using a set of parameters, $\boldsymbol{p}$ that are close to, but not identical to $\boldsymbol{p}_o$:

$$h = h_o + \boldsymbol{J}(\boldsymbol{p} - \boldsymbol{p}_o) \tag{11}$$

where $\boldsymbol{J}$ is a jacobian matrix of m rows of observations and n columns of derivatives of each observation with respect to each of the parameters, with the derivatives calculated using the finite difference method. The objective function, Φ, is then defined by:

$$\phi = (h - h_o - \boldsymbol{J}(\boldsymbol{p} - \boldsymbol{p}_o))^{\mathrm{T}}(h - h_o - \boldsymbol{J}(\boldsymbol{p} - \boldsymbol{p}_o)) \tag{12}$$

where T represents matrix transposition.

The model was calibrated using 47 hydraulic head measurements for the objective function, the positions of which can be seen in Fig. 8. Corresponding calculated head values were obtained from the model nodes located closest to the position of the centre of the well screen in the model domain. The calibration was considered complete when the reduction in Φ was less than 0.005 over four consecutive calibration iterations.

Calibration parameter ranges

The various parameter ranges used for the calibration, shown in Table 1, were determined as follows. Hydraulic conductivity values for the five material types were estimated from particle size distribution curves for samples of aquifer material from the site using the Hazen method (Hazen 1911). For all material types a range of ±50% of the estimated value was used in the calibration.

To estimate groundwater recharge rates for the site, it was assumed that for the sandy topsoil and flat topography found at Brand, the surface runoff of precipitation could be considered to be negligible, and infiltration at the site could be assumed to be equal to the difference between the precipitation and the actual evapotranspiration. The actual evapotranspiration was calculated using the method described by Bagrov (1953), which has been shown to be applicable to Germany (Glugla and Müller 1997). The Bagrov relationship combines mean annual values for corrected precipitation P_{corr}, maximum evapotranspiration based on land use $\mathrm{ET}_{\mathrm{max}}$ and actual evapotranspiration ET_{a}, where

$$\frac{\mathrm{dET}_a}{\mathrm{d}P_{\mathrm{corr}}} = 1 - \left(\frac{\mathrm{ET}_{\mathrm{a}}}{\mathrm{ET}_{\mathrm{max}}}\right)^n \tag{13}$$

The Bagrov parameter, n, which was determined from extensive lysimeter evaluations, describes the water storage characteristics of a soil as a function of the ground cover; for example, coniferous forest, for which evapotranspiration is relatively high, has values of n between around 2.0 and 4.0, while for sandy bare ground, where little evapotranspiration occurs, n has a value of 0.53. Data for precipitation and maximum evapotranspiration from a nearby weather station and the appropriate n values for the ground cover types were used to calculate the potential range of groundwater recharge rates for each of the recharge zones. For zones 7 and 9, where it is thought that the presence of the hanging aquifer significantly reduces recharge to the main aquifer (see Development of the hydrogeological model), a very low maximum recharge was assumed. As zero values are best avoided in the PEST calibration process (Doherty 2004), for zones where the lower limit of the potential recharge range was zero a minimal value of 10 mm/a was used. For zones 5, 6 and 8, where it is thought that recharge from a large area may be focussed by discontinuities in the aquitard of the hanging aquifer, a high maximum recharge was assumed. The upper limit for this was calculated from the volume of recharge intercepted by the hanging aquifer in zone 9 and the ratio of the area of zone 9 to that of zones 5, 6 and 8.

Optimised parameters

When optimising conductivity and recharging simultaneously, it is necessary to consider the problem of

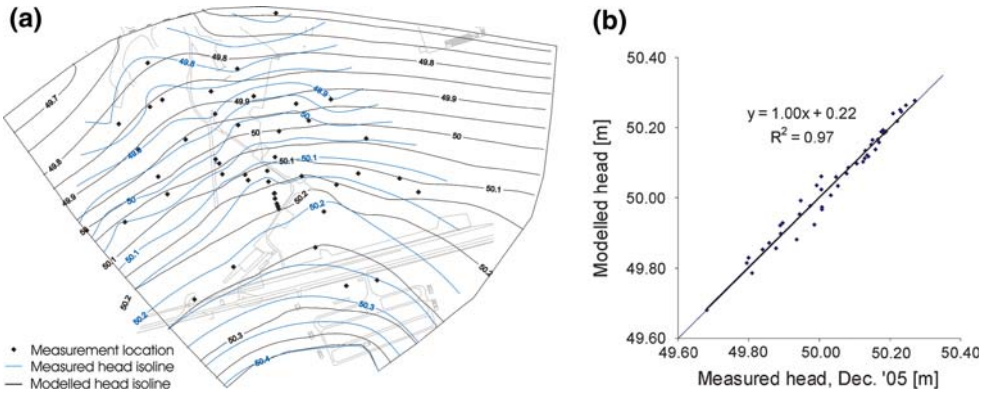

Fig. 8 Optimised model results. **a** Comparison of modelled (*black*) and measured (*blue*) heads showing recharge zonation and monitoring wells used for the calibration. **b** Modelled versus measured head values with linear regression coefficient and y/x = 1.0 line

Table 1 Model parameters included in optimization procedure: calibration parameter ranges and optimised parameter values

Parameter	Category/zone	Initial range of parameter values: minimum–maximum	Optimised parameter value
Hydraulic conductivity ($m\ s^{-1}$)	Fine sand	4.0×10^{-5}–1.2×10^{-4}	1.2×10^{-4}
	Medium sand	3.0×10^{-4}–9.0×10^{-4}	7.0×10^{-4}
	Coarse sand	5.0×10^{-4} –5.0×10^{-3}	1.8×10^{-3}
	Silt	1.0×10^{-5}–4.0×10^{-5}	4×10^{-5}
	Clay	1.0×10^{-6}–4.0×10^{-6}	3×10^{-6}
Recharge (mm/a)	Zone 1 (mixed woodland)	100–250	160
	Zone 2 (landfill)	200–365	200
	Zone 3 (mixed woodland)	100–250	160
	Zone 4 (mixed woodland)	115–300	115
	Zone 5 (low point at edge of perched aquifer)	10–6,000	2,370
	Zone 6 (low point at edge of perched aquifer)	10–6,000	6,000
	Zone 7 (aquitard in unsaturated zone)	10–50	10
	Zone 8 (window in aquitard in the unsaturated zone)	10–6,000	10
	Zone 9 (aquitard in unsaturated zone)	10–50	38
	Zone 10 (scrub/bare ground)	230–360	230

parameter correlation, i.e. that a change in hydraulic conductivity may have the same effect on modelled head values as a change in recharge, which has obvious implications in terms of the uniqueness of the optimised parameter set (Poeter and Hill 1997). While it was seen to be the case during the calibration process that some parameters were strongly correlated, repeating the calibration using different starting values for the parameters yielded the same result for the optimised parameter values, indicating that the calibration process was reaching a global rather than a local minimum for Φ.

The optimised parameter set resulting from the calibration process is shown in Table 1. For the hydraulic conductivities, the optimised parameter values for medium sand, coarse sand and clay lie around the middle of the range used for the calibration, whereas those for fine sand and silt are at the maximum of their allowed ranges. The values for fine and medium sand, which constitute the bulk of the aquifer sediments, compare well with hydraulic conductivities determined from slug tests carried out subsequent to the modelling at various locations where corresponding geological data were available. For fine sand an average value of $1.1 \times 10^{-4} \pm 1.4 \times 10^{-4}$ m/s was determined from slug tests, while the model calibrated value was 1.2×10^{-4} m/s. The slug test determined value for medium sand was $3.0 \times 10^{-4} \pm 1.0 \times 10^{-4}$ m/s, which was the lower limit of the range used for the model calibration. The hydraulic conductivity for medium sand determined in the model calibration was 7×10^{-4} m/s.

For recharge the values for 4 of the 10 zones, namely zones 1, 3, 5 and 9, are well within the parameter ranges, while the remainder tend to the maximum or minimum of their respective allowed ranges. The groundwater recharge rates for the wooded areas are lower than those for bare ground, although the allowed ranges overlap, which is consistent with the assumptions regarding the influence of ground cover. The high values for zones 5 and 6 would appear consistent with the idea of an overflow from the hanging aquifer to the main aquifer discussed earlier.

Optimised model results

The results of the model run with the optimised parameters are shown in Fig. 8. Overall a good agreement between modelled and measured heads was achieved using the optimised parameters, with the objective function $\Phi = 0.024$ m at the end of the calibration process. The maximum absolute error (modelled–measured head) for the 47 observations was 0.06 m. Figure 8a shows a comparison of the modelled and measured head isolines, while in Fig. 8b the modelled heads are shown plotted against the measured, whereby the deviation of the points from the line modelled/measured = 1.0 offers a visual measure of the agreement across the site. It can be seen from Fig. 8b that the errors appear to be randomly distributed as opposed to systematic. The modelled head isolines shown in Fig. 8a are generated from the modelled data at a single elevation, $Z = 48$ m, using all nodes in this plane for the interpolation. As there is a high degree of hydraulic connectivity in the system, the hydraulic heads do not vary with depth within the model domain, and hence the interpolated heads at this arbitrary elevation are considered here as being representative for the whole domain. It should be noted that while the interpolation of measured hydraulic heads is based on 47 values, the interpolation of modelled heads is based on a far larger data set, i.e. head values at all of the model nodes in the lateral plane, which gives rise to some differences between the two sets of isolines.

Results and discussion

The calibration process provided an optimised parameter set for the site model, yielding a good agreement between the model output and measured data for the proposed conceptual site model. The optimised parameters provide support for the assumptions made in the development of the conceptual site model about the way in which the hydrogeological situation at the site is influenced by the hanging aquifer structure. The isolines of the measured head data for the site show an area of divergent flow in the central region of the site where the 50.15 and 50.2 m isolines are strongly curved. As there was no obvious geological feature in the structural model of the saturated zone to account for this behaviour, it was thought that the cause might be the influence of the hanging aquifer in the unsaturated zone, as discussed in the section Development of the conceptual hydrogeological model. In the model simulations it was not possible to reproduce this behaviour without considering high values for groundwater recharge, and the results of the model calibration would seem to support the theory. The levels of recharge for zones 5 and 6, intended to represent the overflow points at the edge of the aquitard in the unsaturated zone, are very high, 2,370 and 6,000 mm/year respectively, while the values for zones 7 and 9, representing the aquitard are very low at 10 and 50 mm/year, respectively. For the area in the centre of the hanging aquifer, zone 8, where it was thought that windows in the aquitard allowed communication with the lower aquifer, the calibrated recharge value of 10 mm/year was comparable to the values for the aquitard areas, suggesting that the communication is less significant than thought.

Concluding remarks

A detailed three-dimensional groundwater flow model was developed for a contaminated field site from a high-resolution geological dataset using the GeoSys/RockFlow finite element code.

A GIS-based conceptual site model was developed based on the geological and hydrogeological data. New software tools were developed and implemented for the translation of the complex conceptual site model into a numerical finite element model. In an initial step, the conceptual model was converted to a geometrical model consisting of point, polyline, surface and volume objects. These were directly derived from the GIS dataset of the conceptual model; thus the geometrical model was an exact reproduction of the original conceptual model. Through these objects, structural information, material properties, boundary conditions and source terms could be conveniently and accurately assigned to the finite element mesh. By mapping elevation information from the layers of the geological model directly to the nodes of the prismatic finite element mesh, the layers of the geological model could be exactly reproduced in the numerical model without the limitations usually encountered due to domain discretisation. Using this approach, the translation of the highly detailed and complex conceptual site model to the numerical model could be achieved with a high degree of accuracy, and without the need for structural simplification.

Calibration of the groundwater flow model using readily available automated calibration software produced a good agreement between modelled and measured hydraulic head data with reasonable values for the optimised parameters. The parameters identified in the calibration process could support hypotheses regarding the hydrogeological situation at the site,

specifically the influence of groundwater recharge on the local flow situation.

The detailed three-dimensional flow model and the identified parameter values provide an essential basis for a reactive transport modelling study, which is being carried out for the site.

Acknowledgments This work is funded by the German Ministry of Education and Research (BMBF) under grants 02WN0352 and 0330512 as a part of the KORA priority program, sub-projects 1.2 and 7.1 and additional funding from the Brandenburgische Boden Gesellschaft für Grundstücksverwaltung und—verwertung mbH (BBG).

References

Bagrov NA (1953) On multi-year average of evapotranspiration from land surface (in Russian). Meteorog i Gridrolog 10:20–25

Bear J (1972) Dynamics of fluids in porous media. Elsevier, New York

Beinhorn M (2005) Contributions to computational hydrology: non-linear flow processes in subsurface and surface hydrosystems. PhD Thesis, Universität Tuebingen, Germany

Carrera J, Neuman S (1986) Estimation of aquifer parameters under transient and steady state conditions. Water Resour Res 22(2):199–242

Chen C (2006) Integrating GIS methods for the analysis of GeoSystems. PhD Thesis, Universität Tuebingen, Germany

Dietrich P and Leven C (2005) Direct push technologies. In: Kirsch R (ed) Groundwater geophysics, Springer, Berlin Heidelberg New York, pp 321–340

Doherty J (2004) PEST. Watermark computing, Corinda, Australia

ESRI (1998) ESRI shapefile technical description. Environmental Systems Research Institute, Inc. http://www.esri.com/library/whitepapers/pdfs/shapefile.pdf

Glugla G and Müller E (1997) Grundwasserneubildung als Komponente der Abflußbildung. Freiburger Schriften zur Hydrologie, 5

Gronewold J (2006) Development of an internet information system for the modelling of natural attenuation processes in groundwater (in German). PhD Thesis, Universität Tuebingen, Germany

Hazen A (1911) Discussion: dams on sand foundations. Transactions, American Society of Civil Engineers 73:199

Hill MC (1992) A computer program (MODFLOWP) for estimating parameters of a transient, three-dimensional, ground-water flow model using nonlinear regression. U.S. Geological Survey Open-File Report 91–484

Hill MC (1998) Methods and guidelines for effective model calibration. U.S. Geological Survey Water-Resources Investigations Report 98–4005

Kalbacher T (2006) Geometric modelling and 3D-visualisation of hydrogeological systems: software design and application. PhD Thesis, Universität Tuebingen, Germany

Kalbacher T, Mettier R, Kosakowski G, Kolditz O (2006) Geometric modelling and object-oriented software concepts applied to a heterogeneous fracture network from grimsel rock laboratory. Comput Geosci (submitted). DOI: 10.1007/s10596-006-9032-8

Kolditz O, Xie M, Kalbacher T, Bauer S, Wang W, McDermott C, Chen C, Beyer C, Gronewold J, Kemmler D, Walsh R, Du Y, Park C-H, Hess M, Bürger C, Delfs J-O (2006) GeoSys/Rockflow—user manual. University of Tuebingen, Center for Applied Geoscience, http://www.uni-tuebingen.de/zag/geohydrology/geosys

Poeter BP, Hill MC (1997). Inverse models: a necessary next step in ground water modeling. Ground Water 35(2):250–260

Robertson PK (1990) Soil classification using the cone penetration test. Can Geotech J 27:151–158

Robertson PK, Campanella RG (1983a) Interpretation of cone penetration tests: Part I: Sand. Can Geotech J 20:719–733

Robertson PK, Campanella RG (1983b) Interpretation of cone penetration tests: Part II: Clay. Can Geotech J 20:734–745

Schulmeister MK et al (2003) Direct-push electrical conductivity logging for high-resolution hydrostratigraphic characterization. Ground Water Monit Remediat 23(3):52–62

Shewchuk JR (1996) Engineering a 2D quality mesh generator and Delaunay triangulator. Applied computational geometry: towards geometric engineering. Springer, Berlin Heidelberg New York, pp 203–222

Wang W and Kolditz O (2006) Object-oriented finite element analysis of thermo-hydro-mechanical (THM) problems in porous media, vol 68. Int J Numer Methods Eng, 16 May 2006 (published online). DOI: 10.1002/nme.1770